PRAMANA
— journal of
physics

Vol. 86, No. 6
June 2016
pp. 1329–1342

Enhancement of nonlinear optical properties of compounds of silica glass and metallic nanoparticle

A GHARAATI[1,*] and A KAMALDAR[1,2]

[1]Department of Physics, Payame Noor University, P.O. Box 19395-3697, Tehran, Iran
[2]Department of Education 1, Shiraz, Iran
*Corresponding author. E-mail: agharaati@pnu.ac.ir

MS received 9 May 2015; accepted 7 July 2015
DOI: 10.1007/s12043-015-1185-3; ***e*Publication:** 23 February 2016

Abstract. The aim of this paper is to introduce a method for enhancing the nonlinear optical properties in silica glass by using metallic nanoparticles. First, the T-matrix method is developed to calculate the effective dielectric constant for the compound of silica glass and metallic nanoparticles, both of which possess nonlinear dielectric constants. In the second step, the Maxwell–Garnett theory is exploited to replace the spherical nanoparticles with cylindrical and ellipsoidal ones, facilitating the calculation of the third-order nonlinear effective susceptibility for a degenerate four-wave mixing case. The results are followed by numerical computations for silver, copper and gold nanoparticles. It is shown, graphically, that the maximum and minimum of the real part of the reflection coefficient for nanoparticles of silver occurs in smaller wavelengths compared to that of copper and gold. Further, it is found that spherical nanoparticles exhibit greater figure-of-merit compared to those with cylindrical or ellipsoidal geometries.

Keywords. Metallic nanoparticles; effective dielectric constant; figure-of-merit.

PACS No. 42.65.−k

1. Introduction

The linear optics of heterogeneous media has been extensively studied, e.g., in refs [1–5]. By utilizing appropriate approximations, various methods for calculating effective dielectric constant can be found in refs [6–10]. Maxwell–Garnett formula is used for inhomogeneities of small volume fraction (VF) (lower than 0.1), and its potential approximations are often applicable [2,5,11]. The nonlinear optical properties of the heterogeneous media have become important in connection with metal colloids and semiconductor crystallites [12–15]. The nonlinear optical properties depend on the size of metallic nanoparticles (MNPs) [16,17]. Flytzanis *et al* have carried out a series of investigations on nonlinear mixing signals produced by a colloidal medium [12,18–21].

It is unfortunate that formal solution to the scattering theorem is only feasible for some specific geometric parameters. Yet, there are analytical solutions to the problems

associated with light scattering, whereby the electromagnetic potentials and fields are expanded by spherical harmonics [22,23]. Such solutions utilize the desirable shape of nanostructures and specific quality-dependent structures such as hot points in gap zones of Papillion antenna, or magnetic response of a two-loop resonator. As such, a sophisticated numerical solution is inevitable to solve Maxwell's equations. One such solution is making use of Gans or Mie–Gans theorem [24], which is applied to solve Maxwell's equation for the spherical particles or infinite-length cylinders.

This paper is aimed at introducing a method for enhancing the nonlinear optical properties in silica glass (SiO_2) by adding MNPs. The first step involves expanding T-matrix method for calculating the effective dielectric constant (EDC) of the compound media, which is composed of silica glass and MNPs, as follows:

$$\varepsilon(\omega) = \varepsilon_1(\omega) + \varepsilon_2(\omega)|E_0|^2, \tag{1}$$

$$\varepsilon'(\omega) = \varepsilon'_1(\omega) + \varepsilon'_2(\omega)\,|E_1|^2\,, \tag{2}$$

where ε_1 and ε_2 represent respectively the linear and nonlinear parts of dielectric constant of silica glass (the host medium), while ε'_1 and ε'_2 are their counterparts for MNPs (the guest medium). In eqs (1) and (2), the applied electric filed and the electric field in the guest medium are denoted by E_0 and E_1, respectively. The shape of nanoparticles is assumed to be spherical. The T-matrix method is scrutinized by replacing the spherical nanoparticles with cylindrical as well as ellipsoidal ones, accompanying the calculation of the effective third-order nonlinear susceptibility coefficient $\bar{\chi}^{(3)}$ (ETNSC). The results from miscellaneous experiments show that although the existence of nanoparticles in silica glass increases the nonlinear reflection coefficient, the figure of merit (FOM) does not increase considerably because in the FOM, which is defined as the ratio of nonlinear refractive index (n) to the two-photon absorption coefficient, the two-photon absorption coefficient also increases. Finally, this study investigates the nonlinear properties of spherical, cylindrical and ellipsoidal MNPs in silica glass for the case of degenerate four-wave mixing (DFWM). Moreover, it shows how these parameters can be increased.

2. Modelling

2.1 *The effective linear dielectric constant compounds of silica glass and spherical MNP*

In the first step, T-matrix method [25] associated with linear dielectric coefficient is used to calculate the EDC and the susceptibility coefficients of a compound medium consisting of silica glass (host) and MNPs (guest). To do so, the host medium is assumed to be a linear medium, in which the refractive index, n, and hence EDCs, depend on the applied wavelength, λ, through the Sellmeier equation,

$$n(\lambda) = \sqrt{1 + \sum\nolimits_{i=1}^{M} A_i \frac{\lambda^2}{\lambda^2 - \lambda_i^2}}, \tag{3}$$

where A_i and λ_i ($i = 1, 2, 3$) are Sellmeier coefficients, which are obtained experimentally [26]. These coefficients are usually expressed for micrometre-order wavelengths. For silica glass $A_1 = 0.696750$, $\lambda_1 = 0.069066$, $A_2 = 0.408218$, $\lambda_2 = 0.115662$, $A_3 = 0.890815$ and $\lambda_3 = 9.900559$.

In the case of linear media, when exploiting the Drude–Lorentz model, the real and imaginary parts of the dielectric constant are considered to be

$$\begin{aligned} \mathrm{Re}\,\varepsilon_1' &= 1 - \frac{\lambda^2}{\lambda_\mathrm{p}^2}, \\ \mathrm{Im}\,\varepsilon_1' &= \frac{g\lambda^3}{\lambda_\mathrm{p}^3 + g^2\lambda_\mathrm{p}\lambda^2}, \end{aligned} \tag{4}$$

with λ_p and g being, respectively, plasma wavelength and conductivity. For spherical MNPs, the effect of electric field E_0 is considered to be E, the Maxwell's field. The model has no restriction regarding the wavelength, but we take 532 nm, because the laboratory results and numerical data are available in this wavelength.

We may write [27,28]

$$E_1 = \frac{3\varepsilon_1}{\varepsilon' + 2\varepsilon_1} E_0, \tag{5}$$

$\left[\varepsilon = \varepsilon(\omega),\ \ \varepsilon' = \varepsilon'(\omega)\right]$. Assuming that there is no interaction between nanoparticles, the average electric field in the heterogeneous medium $\langle E\rangle$ can be written as

$$\langle E\rangle = f\langle E_1\rangle + (1-f)\,\langle E_0\rangle\,, \tag{6}$$

where f is the VF of the nanoparticles. The EDC of the heterogeneous medium $\bar{\varepsilon}$ is the ratio of its average displacement field $\langle D\rangle$ and its average electric field $\langle E\rangle$, that is,

$$\bar{\varepsilon} = \frac{\langle D\rangle}{\langle E\rangle}. \tag{7}$$

Combining eqs (6) and (7), the EDC of the heterogeneous medium can be written as

$$\bar{\varepsilon} = \frac{f\varepsilon'\,\langle E_1\rangle + (1-f)\varepsilon_1\,\langle E_0\rangle}{f\,\langle E_1\rangle + (1-f)\,\langle E_0\rangle}. \tag{8}$$

On the other hand, the average electric field in the nanoparticle can be calculated, using eq. (5), in terms of the average electric field in the medium. Substitution of the result into eq. (8) leads to Maxwell–Garnett equation as

$$\bar{\varepsilon} = \varepsilon\frac{\varepsilon'(1+2f) + 2\varepsilon(1-f)}{\varepsilon'(1-f) + \varepsilon(2+f)}, \tag{9}$$

where an ellipsoidal with a_x, a_y and a_z axes is subjected to an external field of $\vec{E}_0 = (E_{0x}, E_{0y}, E_{0z})$. Following the calculation outlined in refs [27,29], we introduce a parameter $R(s)$ and the depolarization or geometric factors L_i as follows:

$$R(s) = \sqrt{(s+a_x^2)(s+a_y^2)(s+a_z^2)}, \tag{10}$$

$$L_i = \frac{a_x a_y a_z}{2}\int_0^\infty \frac{\mathrm{d}s}{(s+a_i^2)R(s)}, \qquad i = x,\ y, z. \tag{11}$$

Notice that $L_x + L_y + L_z = 1$. For a spherical nanoparticle we have $L_x = L_y = L_z = 1/3$ and for a cylindrical one $L_x = L_y = 1/2$, $L_z = 0$.

The electric field components in the ellipsoidal metallic nanoparticles mentioned above can be given as

$$E_{1j} = \frac{E_{0j}}{1 + L_j[\varepsilon - \varepsilon']/\varepsilon'}, \qquad j = x, y, z\,. \tag{12}$$

Now, assuming the ellipsoidal nanoparticles to have a unidirectional distribution with a small VF, making use of eqs (5)–(9) and ignoring the interaction between the nanoparticles, the EDC of the heterogeneous medium in the directions x, y and z can be obtained as

$$\bar{\varepsilon}_i = \varepsilon' \frac{\varepsilon[f + L_i(1-f)] + \varepsilon'(1-f)(1-L_i)}{\varepsilon L_i(1-f) + \varepsilon'[1 - L_i(1-f)]}, \quad i = x,\ y,\ z\,. \tag{13}$$

2.2 *Reflection coefficient*

The reflection coefficient R is defined [25] as

$$R = \left| \frac{1 - \sqrt{\frac{\varepsilon'}{\varepsilon_1}\left(1 + \frac{f\,\varepsilon_2' A_0^2}{P^2|P|^2\sqrt{\varepsilon' \mathrm{Re}\varepsilon'}}\right)}}{1 + \sqrt{\frac{\varepsilon'}{\varepsilon_1}\left(1 + \frac{f\,\varepsilon_2' A_0^2}{P^2|P|^2\sqrt{\varepsilon' \mathrm{Re}\varepsilon'}}\right)}} \right|^2, \tag{14}$$

where A_0 is the amplitude;

$$P = \frac{1}{3\varepsilon_1}\left[(1-f)\varepsilon' + (2+f)\varepsilon_1\right] \tag{15}$$

and the VF of the nanoparticles in silica glass, f, is assumed to be small because the interaction between the nanoparticles is ignored. We have taken the linear data of silver from ref. [30] and for nonlinear case the typical wavelength is 532 nm [15].

Taking into account the preceding factors [30] and considering the results obtained in ref. [27], the plots regarding $\bar{\varepsilon}$ and R in the wavelength range of 0.2–1.2 μm are depicted in figures 1–3 for $0 < f < 0.1$. They also show the dependency of refractive index on wavelength based on the Sellemier formula. In these figures one can clearly observe where the maximum and minimum of the EDC and R occur in terms of wavelength. For example, in figures 1a and 1b, the real and imaginary parts of the EDC are plotted for a compound of spherical gold nanoparticles and silica glass based on T-matrix method in terms of f and λ. In figure 1a, at $\lambda = 0.5$ μm, the value of the real part of EDC reaches its maximum and it is minimized to 0.4 and in figure 1b, at $\lambda = 0.4$ μm, the value of imaginary part of the EDC reaches its maximum. It should be noted that variation at $0.6 < \lambda < 1.2$ μm for the real and imaginary parts is small and reaches zero.

Similarly, the imaginary part of the EDC can be plotted for different combinations such as spherical gold nanoparticles and silica glass compound using the T-matrix method. The next step involves altering the material of nanoparticles to copper and silver, so that the characteristics of their real and imaginary parts could be examined.

Figures 2a and 2b show the real and imaginary parts of the EDC for a compound of ellipsoidal gold nanoparticles and silica glass based on Maxwell–Garnett model in terms of geometric parameters of nanoparticles, L_i, and wavelength.

Figures 3a and 3b illustrate the real and imaginary parts of the reflection coefficient, R, for a compound of spherical gold nanoparticles and silica glass based on T-matrix method in terms of VF of nanoparticles and wavelength.

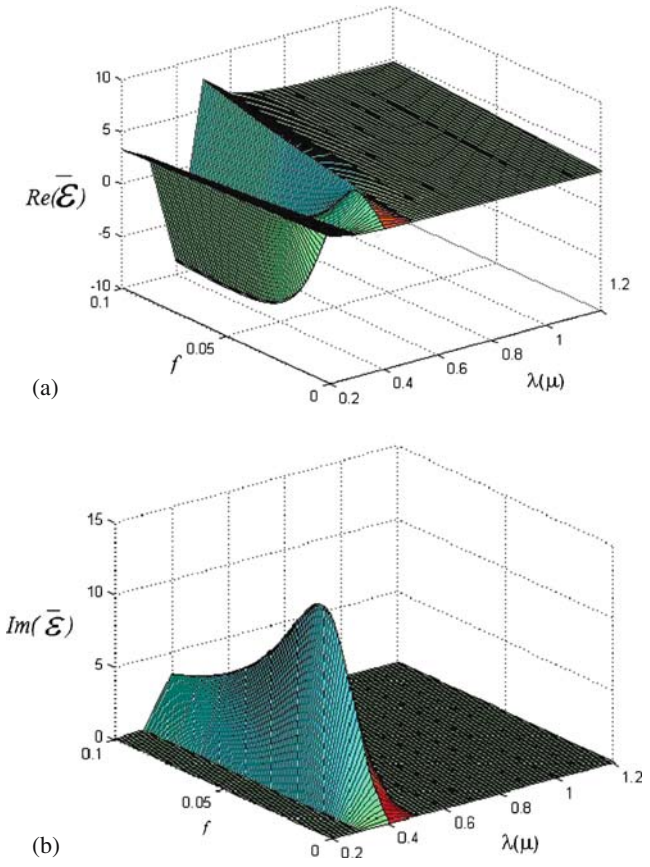

Figure 1. The EDC after the addition of spherical gold nanoparticles to the silica glass using T-matrix method. (**a**) Real part and (**b**) imaginary part.

Substitution of gold nanoparticles with copper nanoparticles yields similar results. But, when silver nanoparticles are used as guest ones, the value of the real part of reflection coefficient reaches its maximum at $\lambda = 0.35\ \mu$m and minimum at $\lambda = 0.55\ \mu$m. So, it can be concluded that for silver the maximum and minimum points of reflection coefficient occur at shorter wavelengths.

Similarly, the imaginary part of the reflection coefficient can be plotted for copper nanoparticles in silica glass compound. Again, at $\lambda = 0.8\ \mu$m, the value of the imaginary part of reflection coefficient reaches its maximum ($R = 0.5$). It occurs at shorter wavelengths (0.6 μm) when silver rather than copper is used.

2.3 *DFWM in silica glass and nanoparticle compounds*

In this section, parallel to the study done in [25,27], we calculate DFWM in silica glass and nanoparticle compound for a compound heterogeneous medium consisting of silica glass (host) and ellipsoidal gold, silver or copper MNPs (guest), which are spread in one

direction in nonlinear dielectric medium. Both the host and the guest have nonlinear optical properties.

The electric field components in an ellipsoidal along x-, y- and z-axes are as follows:

$$E_{i\,k} = \frac{E_{0k}}{1 + L_k(\varepsilon_{2k}^{\text{non}} - \varepsilon_{1k}^{\text{non}})/\varepsilon_{1k}^{\text{non}}}, \quad k = x,\, y,\, z, \tag{16}$$

where i represents the interior of the guest medium, the term $\varepsilon_{1k}^{\text{non}}$ $(k = x, y, z)$ is the nonlinear EDC of the host and $\varepsilon_{2k}^{\text{non}}$ $(k = x, y, z)$ is the nonlinear EDC of the guest. The nonlinear EDC of the ellipsoidal nanoparticles of the guest is

$$\varepsilon_{2k}^{\text{non}}(\omega) = \varepsilon_1'(\omega) + \varepsilon_2' \left|E_{ik}\right|^2, \quad k = x, y, z. \tag{17}$$

If ε_1' and ε_2' are respectively the linear and nonlinear EDCs of the guest nanoparticles, the nonlinear EDC of the host medium will be

$$\varepsilon_{1k}^{\text{non}}(\omega) = \varepsilon_1(\omega) + \varepsilon_2 \left|E_{0k}\right|^2, \quad k = x, y, z, \tag{18}$$

where ε_1 and ε_2 are respectively the linear and nonlinear EDCs of the host nanoparticles. E_{ik} is the component of the guest's electric field and $E_{0\,k}$ is the same one for the exerting

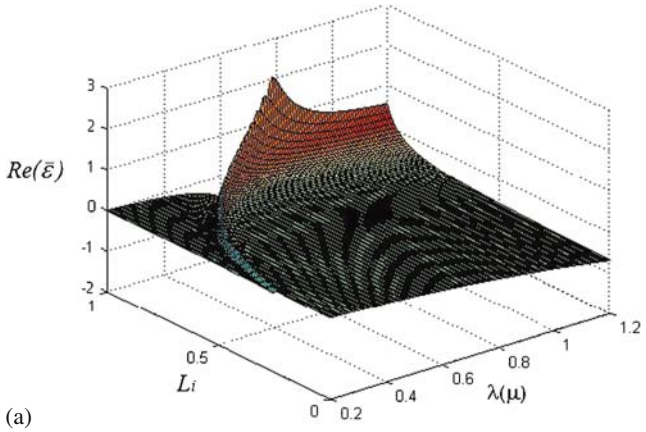

(a)

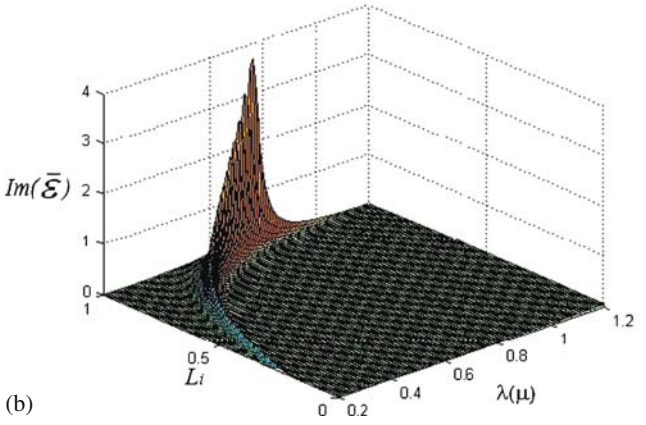

(b)

Figure 2. The same as figure 1 but for ellipsoidal gold nanoparticles.

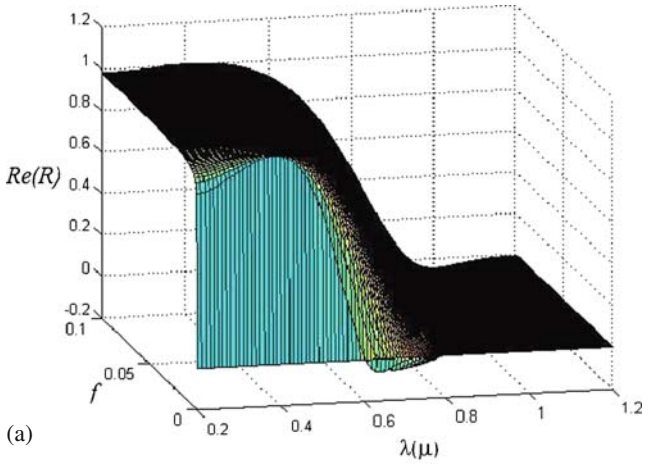

(a)

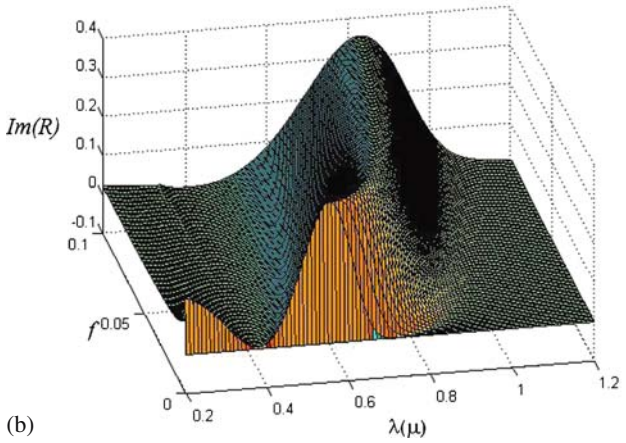

(b)

Figure 3. The reflection coefficient after adding spherical gold nanoparticles to the silica glass using T-matrix method. (**a**) Real part and (**b**) imaginary part.

field. Calculations and simplifications in the x direction show that

$$E_{ix} = \frac{\varepsilon_{1x}^{\text{non}}}{\varepsilon_{1x}^{\text{non}} + L_x(\varepsilon_{2x}^{\text{non}} - \varepsilon_{1x}^{\text{non}})} E_{0x}. \tag{19}$$

But, on the other hand,

$$E_{ix} = x' E_{0x}. \tag{20}$$

For converting the spherical formulation represented by Agarwal *et al* [25] to the ellipsoidal ones, similar calculations should be performed [25,27].

$$x' = \frac{\varepsilon_{1x}^{\text{non}}}{\varepsilon_{1x}^{\text{non}} + L_x\left(\varepsilon_{2x}^{\text{non}} - \varepsilon_{1x}^{\text{non}}\right)}. \tag{21}$$

Hence,

$$D = \varepsilon_{2k}^{\text{non}}(\omega) E. \tag{22}$$

But, when the electric field of the nonlinear signal is

$$E_s^{\mathrm{NL}} = \frac{-4\pi}{\varepsilon(\omega_j) + 2\varepsilon_0(\omega_j)} P^{\mathrm{NL}}, \tag{23}$$

where

$$\begin{aligned} P^{\mathrm{NL}} &= \chi^{(3)}_{112} x_1'^2 x_2'^* E_{10} E_{10} E_{20}^*, \\ x_j' &= \frac{3\varepsilon_0(\omega_j)}{\varepsilon(\omega_j) + 2\varepsilon_0(\omega_j)}, \quad j = 1, 2 \text{ and } s. \end{aligned} \tag{24}$$

E_s^{NL} and D_s^{NL} in terms of the T-matrix method can be expressed as follows [25]:

$$D_s^{\mathrm{NL}} = \varepsilon_0 \langle E_s^{\mathrm{NL}} \rangle + 4\pi \langle T^{(3)}_{112} \rangle E_{10} E_{10} E_{20}^*. \tag{25}$$

By substituting P^{NL} in eq. (23)

$$E_s^{\mathrm{NL}} = \frac{-4\pi}{\varepsilon(\omega_j) + 2\varepsilon_0(\omega_j)} \chi^{(3)}_{112} x_1'^2 x_2'^* E_{10} E_{10} E_{20}^*. \tag{26}$$

From eqs (23)–(26), it can be inferred that the average electric field of this nonlinear signal is as the one below.

$$E_s^{\mathrm{NL}} = \frac{-4\pi}{3\varepsilon_0(\omega_j)} \chi^{(3)}_{112} x_s' x_1'^2 x_2'^* E_{10} E_{10} E_{20}^*, \tag{27}$$

$$\begin{aligned} \langle E_s^{\mathrm{NL}} \rangle = 4\pi (&\langle G T^{(3)}_{sss} \rangle |E_{s0}|^2 E_{s0} + \langle G T^{(3)}_{s11} \rangle |E_{10}|^2 E_{s0} \\ &+ \langle G T^{(3)}_{s22} \rangle |E_{20}|^2 E_{s0} + \langle G T^{(3)}_{112} \rangle E_{10} E_{10} E_{20}^*), \end{aligned} \tag{28}$$

where G is an integral operator [25].

By comparing eqs (27) and (28), $\langle G T^{(3)}_{112} \rangle$ can be written as

$$\langle G T^{(3)}_{112} \rangle = -\frac{1}{3\varepsilon_0(\omega_j)} \chi^{(3)}_{112} x_s' x_1'^2 x_2'^*, \tag{29}$$

and the electric displacement in signal frequency ω_s, where $\omega_s = \omega_1 = \omega_2$, is written as [25]

$$D_s^{\mathrm{NL}} = \varepsilon_0 \langle E_s^{\mathrm{NL}} \rangle + 4\pi \langle T^{(3)}_{112} \rangle E_{10} E_{10} E_{20}^*. \tag{30}$$

By substituting E_s^{NL} in eq. (30), we get

$$D_s^{\mathrm{NL}} = 4\pi \left[\varepsilon_0 \left(-\frac{1}{3\varepsilon_0} \chi_{112}^{(3)} x_s' x_1'^2 x_2'^* \right) + \langle T_{112}^{(3)} \rangle \right] E_{10} E_{10} E_{20}^*, \tag{31}$$

D_s^{NL} can also be expressed as

$$D_s^{\mathrm{NL}} = \varepsilon E_s^{\mathrm{NL}} + 4\pi P^{\mathrm{NL}}. \tag{32}$$

By substituting E_s^{NL} and P^{NL} from eqs (24) and (27) into eq. (32) D_s^{NL} can be written as

$$\begin{aligned} D_s^{\mathrm{NL}} = {} & \varepsilon(\omega_j) \left(\frac{-4\pi}{3\varepsilon_0(\omega_j)} \chi_{112}^{(3)} x_s' x_1'^2 x_2'^* E_{10} E_{10} E_{20}^* \right) \\ & + 4\pi \chi_{112}^{(3)} x_1'^2 x_2'^* E_{10} E_{10} E_{20}^*, \end{aligned} \tag{33}$$

and by comparing eqs (30) and (31) with eq. (33) an explicit expression is obtained for $\langle T_{112}^{(3)} \rangle$

$$\langle T_{112}^{(3)} \rangle = \chi_{112}^{(3)} x_s' x_1'^2 x_2'^*. \tag{34}$$

Similar to the case of spherical nanoparticles, the average of T-matrices for a heterogeneous medium of VF, f consisting of ellipsoidal nanoparticles can be written as follows [25]:

$$\langle T_j^{(1)} \rangle = f(\varepsilon(\omega_j) - \varepsilon_0(\omega_j)) x_j, \tag{35}$$

$$\langle T_j^{(1)} \rangle = f(\varepsilon(\omega_j) - \varepsilon_0(\omega_j)) x_j, \tag{36}$$

$$\langle T_{112}^{(3)} \rangle = \chi_{112}^{(3)} f x_s' x_1'^2 x_2'^*, \tag{37}$$

$$\langle G T_{112}^{(3)} \rangle = -\frac{1}{3\varepsilon_0(\omega_j)} f x_s' x_1'^2 x_2'^*. \tag{38}$$

Finally, the ETNSC is

$$\bar{\chi}_{112}^{(3)} = \chi_{112}^{(3)} f \frac{\left| x_1' \right|^2 x_2'^2}{\left| 1 + f(x_1' - 1) \right|^2 [1 + f(x_2' - 1)]^2}. \tag{39}$$

Table 1. Variations of FOM in silica glass after the addition of different cylindrical MNPs for a DFWM at $\lambda = 532$ nm.

Composite	f	$\mathrm{Re}\bar{\chi}_{211}^{(3)}$(esu)	$\mathrm{Im}\bar{\chi}_{211}^{(3)}$(esu)	$\lvert\bar{\chi}_{211}^{(3)}\rvert$ (esu)	FOM
Silica and Au	0.08	-2.49×10^{-7}	4.10×10^{-7}	4.80×10^{-7}	0.93
Silica and Cu	0.08	-1.09×10^{-8}	1.33×10^{-8}	1.72×10^{-8}	0.03
Silica and Ag	0.08	4.93×10^{-12}	1.11×10^{-13}	4.93×10^{-12}	3.25
Silica and Au	0.06	-1.45×10^{-7}	2.72×10^{-7}	3.09×10^{-7}	0.90
Silica and Cu	0.06	-7.07×10^{-9}	9.09×10^{-9}	1.15×10^{-8}	1.08
Silica and Ag	0.06	3.37×10^{-12}	7.59×10^{-14}	3.37×10^{-12}	3.34

Table 2. Variations of FOM in silica glass after the addition of different spherical MNPs for a DFWM at $\lambda = 532$ nm.

Composite	f	$\mathrm{Re}\bar{\chi}^{(3)}_{211}$(esu)	$\mathrm{Im}\bar{\chi}^{(3)}_{211}$(esu)	$\left\vert\bar{\chi}^{(3)}_{211}\right\vert$(esu)	FOM
Silica and Au	0.08	-2.71×10^{-6}	-2.05×10^{-6}	3.39×10^{-6}	0.32
Silica and Cu	0.08	-1.25×10^{-7}	2.45×10^{-8}	1.28×10^{-7}	0.16
Silica and Ag	0.08	2.99×10^{-11}	7.07×10^{-13}	2.99×10^{-11}	3.69
Silica and Au	0.06	-2.13×10^{-6}	-1.29×10^{-6}	2.49×10^{-6}	0.54
Silica and Cu	0.06	-8.45×10^{-8}	2.07×10^{-8}	8.70×10^{-8}	0.35
Silica and Ag	0.06	2.03×10^{-11}	4.79×10^{-13}	2.03×10^{-11}	3.8

Experiments and calculations show that the nonlinear refractive index will increase after the addition of MNPs and we can conclude that the 2-photon absorption coefficient will also increase [9]. Thus, the FOM will not change due to the following equation:

$$\mathrm{FOM} = \frac{\left\vert\chi^{(3)}\right\vert}{4\pi\,\mathrm{Im}(\chi^{(3)})}. \tag{40}$$

When materials are used, FOM becomes significant. High values of FOM are needed for the systems, all of which are optical systems. In tables 1 and 2, the influence of the addition of different nanoparticles with different shapes is shown. They are for the case of small VFs (0.06 and 0.08) in DFWM at $\lambda = 532$ nm [15,25]. As can be observed, the highest value of FOM is attributed to the silver nanoparticles.

Tables 1 and 2 show the influence of adding different cylindrical and spherical nanoparticles. They are for the cases with small VFs (0.06 and 0.08) in a DFWM, at $\lambda = 532$ nm. Moreover, it is shown that the highest value of FOM is related to silver nanoparticles. The remarkable conclusion after comparing tables 1 and 2 is that the spherical nanoparticles yield larger values of FOM.

Figures 4a–4c and 5a–5c respectively show the variations of the magnitude, real and imaginary parts of ETNSC ($\bar{\chi}^{(3)}_{112}$) after adding ellipsoidal nanoparticles of gold and silver for a DFWM at $\lambda = 532$ nm on the basis of L and f. Here, the values of ETNSC are expressed in terms of esu.

The variations of the magnitude of ETNSC ($\bar{\chi}^{(3)}_{112}$) for silica glass and ellipsoidal copper nanoparticles can be plotted in the same way. For this case, at $f = 0.02$ the magnitude of ETNSC reaches its maximum. By increasing f to 0.1, the ETNSC approximately remains constant and close to zero. The behaviour of the real and imaginary parts of ETNSC is the same as the magnitude.

Using eq. (45) the FOM for gold nanoparticles in silica glass can be calculated as shown in figure 6. The maximum FOM occurrs at $f = 0.035$ for geometric parameters of 0.28, 0.53 and 0.8.

In this paper, results of the T-matrix method and the experimental ones for different composite glasses are compared well [8,31].

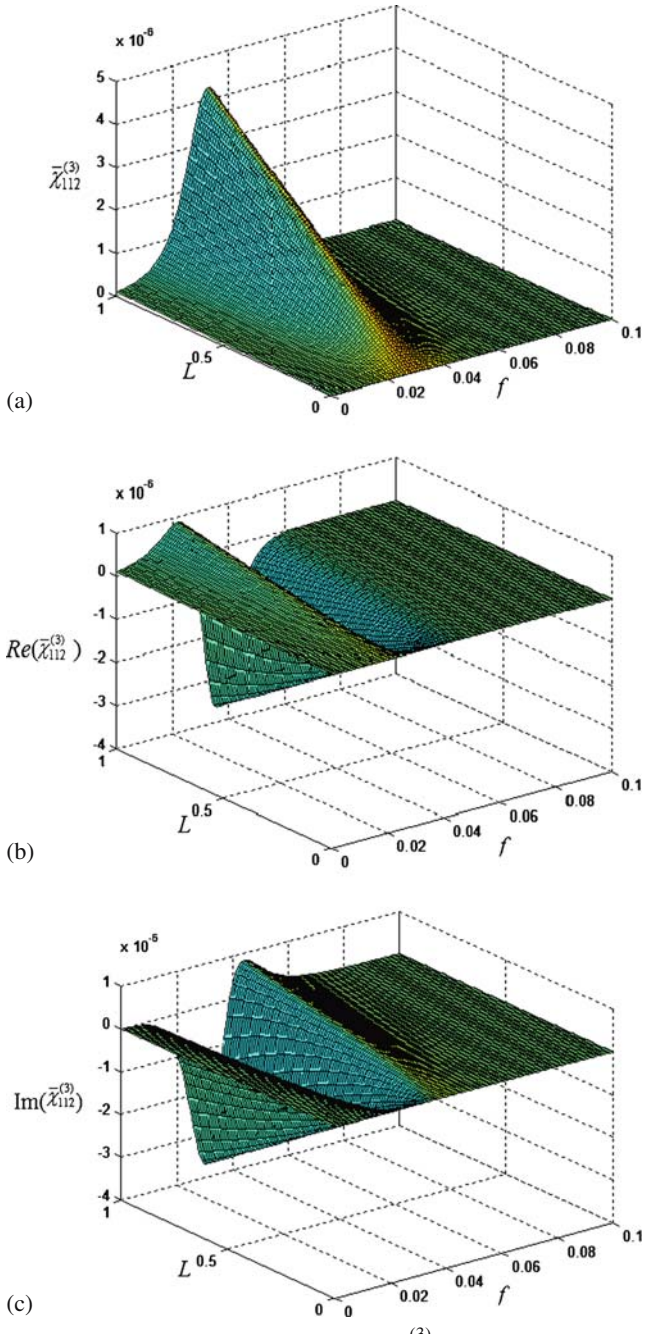

Figure 4. Variations of the ETNSC ($\bar{\chi}^{(3)}_{112}$) after the addition of gold ellipsoidal nanoparticles for a DFWM at $\lambda = 532$ nm on the basis of L and f. (**a**) Magnitude, (**b**) real part and (**c**) imaginary part.

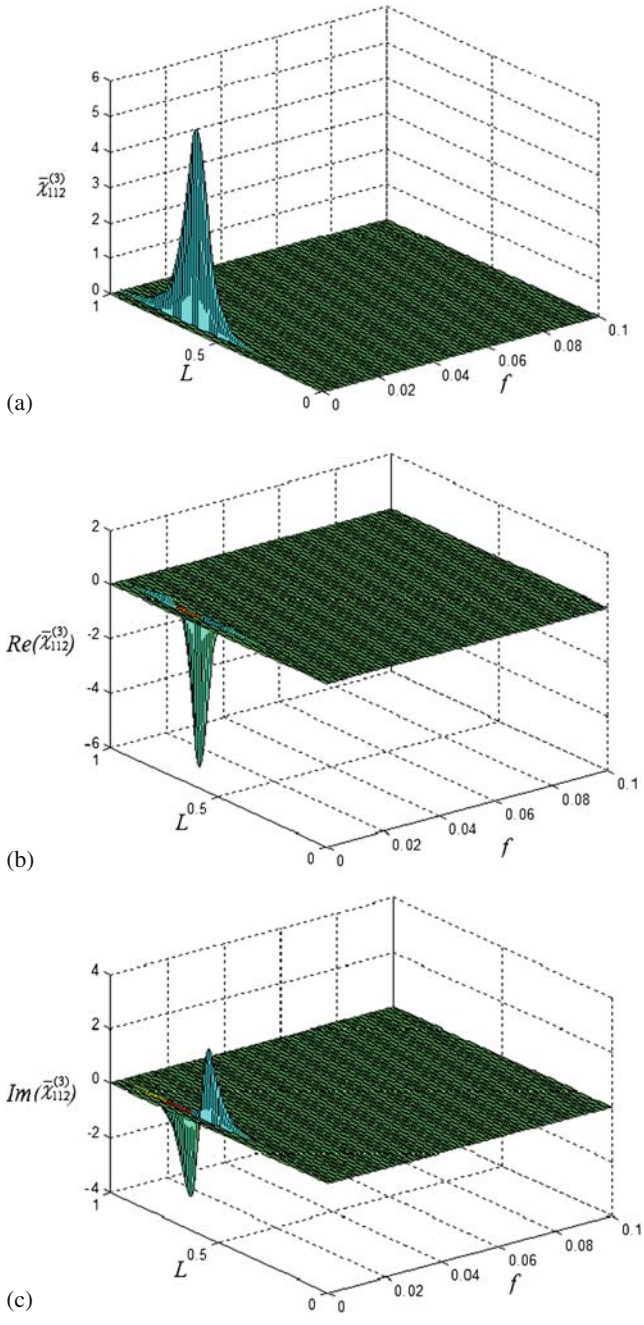

Figure 5. The same as figure 4, but for the silver ellipsoidal nanoparticles.

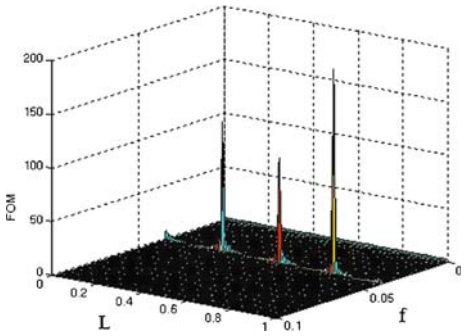

Figure 6. Variations of the FOM after the addition of silver ellipsoidal nanoparticles for a DFWM at 532 nm wavelength on the basis of L and f.

3. Conclusions

In this research, the physics of enhancement of nonlinear properties of silica glass by adding metallic nanoparticles was investigated by utilizing local fields, plasma wavelength and Drude model. Metallic nanoparticles such as gold, silver or copper were shown to have negative effective dielectric constant in the real part and small imaginary one in the optical and infrared wavelength range. Thus, at this special wavelength, which is called plasma wavelength, the local field reaches its maximum, affecting the existing guest metallic nanoparticles in silica glass, which yields an increase in nonlinear properties of the newly created heterogeneous medium. It is assumed that the metallic nanoparticles are spread randomly in the medium. Increasing the intensity of the external field causes an increase in the nonlinearity property of the heterogeneous medium. All the governing models which describe the linear and nonlinear properties of heterogeneous medium are presented upon no-interaction circumstance between nanoparticles ($f < 0.1$).

The model proposed for nanoparticles with different shapes was expanded, and T-matrix method was used to derive the effective dielectric constant and third-order nonlinear susceptibility coefficient ($\bar{\chi}^{(3)}$) of the compound of ellipsoidal nanoparticles and silica glass. The required relations can be derived for extreme cases of spherical, cylindrical and ellipsoidal nanoparticles. The effects of changing the shape of nanoparticles were investigated for silica–gold, silica–silver and silica–copper, and it was shown that the effective third-order nonlinear susceptibility coefficient ($\bar{\chi}^{(3)}$) and figure-of-merit were larger for spherical nanoparticles than those for cylindrical ones. Considering tables 1 and 2 and the information gathered, it can be inferred that adding metallic nanoparticles increases nonlinear properties of a heterogeneous material. Because of the high nonlinear properties of these materials, even if only small volume fractions are used, high increases in those properties can be resulted.

Acknowledgements

This work has been financially supported by the Payame Noor University (PNU), I.R. of Iran under the Dr Abdolrasoul Gharaati grant.

References

[1] I D Rukhlenko, W Zhu, M Premaratne and G P Agrawal, *Opt. Express* **20(24)**, 26275 (2012)
[2] C Z Fan, J P Huang and K W Yu, *J. Phys. Chem. C* **113**, 18504 (2009)
[3] I Webman, J Jortner and M H Cohen, *Phys. Rev. B* **15**, 5712 (1977)
[4] W Lamb, D M Wood and N W Ashcroft, *Phys. Rev. B* **21**, 2248 (1980)
[5] G S Agarwal and R Inguva, *Phys. Rev. B* **30**, 6108 (1984)
[6] S Sharma, D Mohan and S Ghoshal, *Opt. Commun.* **28**, 2923 (2008)
[7] D A G Bruggeman, *Ann. Phys.* **24**, 636 (1935)
[8] A Zakery and H Shahmirzaee, *J. Phys. D: Appl. Phys.* **41(22)**, 225106(1-7) (2008)
[9] A Zakery and H Shahmirzaee, *Phys. Lett. A* **361**, 484 (2007)
[10] N Boris, A Vitaly and G Nikolia, *Langmuir* **24(16)**, 8964 (2008)
[11] J C M Garnett, *Phil. Trans. R. Soc. London Ser. A* **203**, 385 (1904)
[12] K C Rustagi and C Flytzanis, *Opt. Lett.* **9**, 344 (1984)
[13] J Yumoto, S Fukushima and K Kubodera, *Opt. Lett.* **12**, 832 (1987)
[14] Y Liu, D Li, R Y Zhu and G J You, *Appl. Phys. B: Lasers and Optics* **76**, 435 (2003)
[15] Y Takeda, V T Gritsyna, N Umeda, C G Lee and N Kishimoto, *Nucl. Instrum. Methods B* **148**, 1029 (1999)
[16] S Jafari, H Shahmirzaee and A Gharaati, *J. Nonlinear Opt. Phys. Mat.* **21**, 1250020(1-23) (2012)
[17] K Fukumi, A Chayahara, K Kadono, T Sakaguchi, Y Horino, M Miya, K Fujii, J Hayakawa and M Satou, *J. Appl. Phys.* **75(6)**, 3076 (1994)
[18] P Roussignol, D Ricard, J Lukasik and C Flytzanis, *J. Opt. Soc. Am. B* **4(5)**, 5 (1987)
[19] R J Gehr, G L Fischer and R W Boyd, *J. Opt.* **14(9)**, 2310 (1997)
[20] E Cattaruzza, G Battaglin, F Gonella and R Polloni, *Appl. Surf. Sci.* **254**, 1017 (2007)
[21] A E Neeves and M H Birnboim, *Opt. Soc. Am. B* **6**, 787 (1989)
[22] G Kaur, F Wang, Y M Yiu, D W Shoessmith, M Zinke-Allmang, T Sham and Z Ding, *J. Mater. Sci. Mater. Electron.* **20**, 164 (2009)
[23] D D Smith, Y Yoon, R W Boyd, J K Campbell, L A Baker, R M Crooks and M George, *J. Appl. Phys.* **86**, 6200 (1999)
[24] U Kreibig, *Phys. Unserer Zeit.* **39(6)**, 281 (2008)
[25] G S Agarwal and S D Gupta, *Phys. Rev. A* **38(11)**, 5678 (1988)
[26] R Th Kersten, *Einführung in die Optische Nachrichtentechnik* (Springer Verlag, Berlin, Heidelberg, New York, 1983)
[27] A Zakery and H Shahmirzaee, *Phys. Lett. A* **361(6)**, 484 (2007)
[28] J R Reitz, F J Milford and R W Christy, *Foundation of electromagnetic theory*, 4th edn (Addison-Wesley Pub. Co, Reading, Mass, USA, 1992)
[29] J A Stratton, *Electromagnetic theory* (John Wiley & Sons Inc., Hoboken, New Jersey, 2007)
[30] P B Johnson and R W Christy, *Phys. Rev. B* **6(12)**, 4370 (1972)
[31] *J. Phys. D: Appl. Phys.* Volume 41 Number 22